DISCRETE AND CONTINUOUS
DYNAMICAL SYSTEMS SERIES S
Volume **4**, Number **6**, December **2011**

doi:10.3934/dcdss.2011.4.1499

pp. **1499–1509**

A COMPUTATIONAL STUDY OF AVIAN INFLUENZA

Shu Liao

College of Mathematics and Statistics
Chongqing Technology and Business University
Chongqing 400067, China

Jin Wang

Department of Mathematics and Statistics
Old Dominion University
Norfolk, VA 23529, USA

Jianjun Paul Tian

Department of Mathematics
College of William and Mary
Williamsburg, VA 23187, USA

Abstract. We propose a PDE model and conduct numerical simulation to study the temporal and spatial dynamics of the Avian Influenza, and investigate its epidemic and possibly pandemic effects in both the bird and human populations. We present several numerical examples to carefully study the population dynamics with small initial perturbations. Our results show that in the absence of external controls, any small amount of initial infection would lead to an outbreak of the influenza with considerably high death rates in both birds and human beings.

1. **Introduction.** Over the past decades, Avian Influenza (or bird flu) has become a serious infectious disease that causes tremendous media attention [11, 12]. Outbreaks of Avian Influenza of subtype H5N1 have been frequently reported in Asia, Russia, the Middle East, Europe and Africa since 1997. Although its infection in human beings is limited so far, the pandemic effects on bird population and domestic bird industry are significant. Despite many research efforts that have been devoted to the study of Avian Influenza [3, 7, 8], a number of issues still remain unclear in the processes of infection and spread. Furthermore there are many questions to be answered both genetically and ecologically. One particularly interesting question, which is also of great concern to human beings, is whether a sufficiently small amount of infected birds can lead to a pandemic in both bird and human populations. To seek an answer, we have to take into consideration of both the Low Pathogenic Avian Influenza (LPAI) and High Pathogenic Avian Influenza (HPAI). While only does HPAI pose serious threats to human health, LPAI is common in wild birds and poultry, and can transform to HPAI under certain conditions [7].

Recently, Tian and his coworkers [2, 9] developed mathematical models, which consist of systems of several ordinary differential equations (ODEs), to study the interactions between LPAI and HPAI, and their combined effects on bird and human

2000 *Mathematics Subject Classification.* 65M06, 92D30.
Key words and phrases. LPAI, HPAI, numerical PDE.

populations. However, only the time evolution of the infection was discussed in these models, and spatial dynamics was not considered. To overcome this limitation, we propose in this paper a system of partial differential equations (PDEs) which models the spatial variance by adding a diffusion term (i.e., second-order spatial derivative) to each equation. This approach is similar to the work [6] in modeling the spatial spread of West Nile virus infection. Based on this PDE model, we conduct numerical simulation to carefully investigate both the temporal and spatial dynamics of the Avian Influenza, and discuss its epidemic and possibly pandemic behaviors among bird and human populations. In particular, we represent the effects of small initial infections by adding small perturbations to the initial configuration, and study the subsequent long-term dynamics of the system.

The remainder of this paper is organized as follows. In Section 2, the PDE model is presented. In Section 3, the numerical method to be applied to the PDE system is described. In Section 4, results from the numerical simulations with various initial profiles are discussed. Finally, a conclusion is drawn and a brief discussion for future study is made.

2. **PDE model.** We present the PDE model for the influenza in both the avian and human populations. The model is based on the following diagram [10].

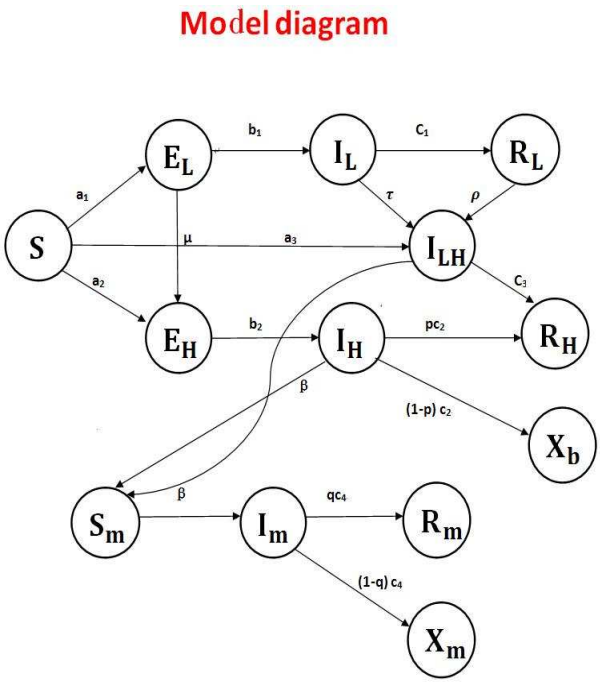

Here we use the subscripts L and H to distinguish the LPAI and HPAI, respectively. The subscript m refers to the human population. Essentially, the upper part of the diagram illustrates the evolution of the influenza in birds, and the lower part illustrates that among people. The notations are further explained below:

- S, the set of susceptible birds or people
- R, the set of recovered birds or people
- E, the set of latent birds

- I, the set of infected birds or people
- X, the set of dead birds or people

Our PDE system consists of nonlinear parabolic equations to describe the infection dynamics. The time derivatives measure the rate of change for each population set, and the diffusion terms model the spread of the infection. The nonlinear terms in these equations occur due to the interaction between different population sets. The first nine equations are concerned with the bird part, and the last four equations are for the human part. Note that we have introduced the letter N to denote the total population which is assumed to be a constant.

$$\frac{\partial S}{\partial t} = -a_1 \frac{I_l}{N} S - a_2 \frac{I_h}{N} S - a_3 \frac{I_l h}{N} S + \varepsilon \nabla^2 S \tag{1}$$

$$\frac{\partial E_l}{\partial t} = a_1 \frac{I_l}{N} S - b_1 E_l - \mu E_l + \varepsilon \nabla^2 E \tag{2}$$

$$\frac{\partial E_h}{\partial t} = a_2 \frac{I_h}{N} S - b_2 E_h + \mu E_l + \varepsilon \nabla^2 E_h \tag{3}$$

$$\frac{\partial I_l}{\partial t} = b_1 E_l - \tau \frac{I_l I_h}{N} - C_1 I_l + \varepsilon \nabla^2 I_l \tag{4}$$

$$\frac{\partial I_h}{\partial t} = b_2 E_h - C_2 I_h + \varepsilon \nabla^2 I_h \tag{5}$$

$$\frac{\partial I_{lh}}{\partial t} = \tau \frac{I_l I_h}{N} + a_3 \frac{I_{lh}}{N} S + \rho \frac{I_h}{N} R_l - C_3 I_{lh} + \varepsilon \nabla^2 I_{lh} \tag{6}$$

$$\frac{\partial R_l}{\partial t} = C_1 I_l - \rho \frac{I_h}{N} R_l + \varepsilon \nabla^2 R_l \tag{7}$$

$$\frac{\partial R_h}{\partial t} = P C_2 I_h + C_3 I_{lh} + \varepsilon \nabla^2 R_h \tag{8}$$

$$\frac{\partial X_b}{\partial t} = (1 - P) C_2 I_h \tag{9}$$

$$\frac{\partial S_m}{\partial t} = -\beta \frac{I_h + I_{lh}}{N} S_m + D \nabla^2 S_m \tag{10}$$

$$\frac{\partial I_m}{\partial t} = \beta \frac{I_h + I_{lh}}{N} S_m - C_4 I_m + D \nabla^2 I_m \tag{11}$$

$$\frac{\partial R_m}{\partial t} = q C_4 I_m + D \nabla^2 R_m \tag{12}$$

$$\frac{\partial X_m}{\partial t} = (1 - q) C_4 I_m \tag{13}$$

There are various parameters which appear in the above equations, representing the LPAI and HPAI infection rates, the death and recovery rates, and the infectious and latent periods, etc. [9]. The values of these parameters are provided in Table 1. Most of these parameters can be found in the literature [3, 4, 5]; others have been determined so as to match the statistical data. For convenience of discussion, we have chosen to normalize the total population to N=1, so that each population set is represented by a corresponding fraction.

$a_1 = 0.45$	$b_1 = \frac{1}{2}$
$a_2 = 2.1$	$c_1 = \frac{1}{6}$
$b_2 = \frac{1}{10}$	$c_2 = \frac{1}{9}$
$a_3 = 0.4$	$c_3 = \frac{1}{2}$
$P = 0.1$	$\tau = 1.3$
$\mu = 0.01$	$\beta = 0.025$
$c_4 = \frac{1}{7}$	$q = 0.51$
$D = 1.0$	$\rho = 1.2$

TABLE 1. Parameter values for the PDE system

3. **Numerical method.** In this project, we assume the spatial domain is one-dimensional: $0 \leq x \leq Ł$. This can be treated as an approximation to a two-dimensional area in the xy-plane where the spatial variance in the vertical (y) direction is ignored. Although this is a much simplified case, the methodology and results from this project will provide a solid background for future study on two-dimensional and three-dimensional modeling, which are expected to generate more practical results.

Since the equations in the PDE system are of parabolic type, a simple choice of numerical method is the FTCS scheme [1] (Forward difference in Time and Centered difference in Space). For illustration, consider a general parabolic-type equation in the form:

$$\frac{\partial u}{\partial t} + C(t, x, u)\frac{\partial u}{\partial x} = \mu \frac{\partial^2 u}{\partial^2 x} \tag{14}$$

where μ is a constant and c is a function of t, x and u. The FTCS algorithm applied to this generic equation yields:

$$\frac{u_j^{n+1} - u_j^n}{\triangle t} + C(t_n, x_j, u_j^n)\frac{u_{j+1}^n - u_{j-1}^n}{2\triangle x} = \mu \frac{u_{j+1}^n - 2u_j^n + u_{j-1}^n}{(\triangle x)^2} \tag{15}$$

where the subscript j denotes the spatial grid and the superscript n refers to the time step. This is an explicit, one-step scheme with a truncation error of $O[\triangle t, (\triangle x)^2]$. With this method, no iterative scheme is needed and no start-up procedure is necessary, thus it is straightforward to implement. We have found this method stable with reasonably small $\triangle t$ when applied to our PDE system.

4. **Computational results.**

4.1. **Validity tests.** As mentioned before, the authors in [2, 9] developed ODE models to study the time evolution of avian influenza. Those models differ from the PDE model we consider in that the spatial dynamics is not present. Nevertheless, their results provide a way to justify the validity of our numerical calculation in terms of the time evolution behaviors. To compare the results, we set uniform initial conditions so as to minimize the spatial variance, and we plot the solution curves at a fixed spatial point (say, the midpoint of the domain) with respect to time. We expect that when ε is sufficiently small, the diffusion effect is close to being negligible and our results will match those from the ODE model. With increased

values of ε, however, our results are expected to exhibit different behaviors from those ODE results, showing the presence of the diffusion effects. We only consider the bird population in these tests for ease of comparison.

4.1.1. We first set $\varepsilon = 0.001$, representing a very small diffusive effect, and set the initial conditions all equal zero except the following: $S = 0.92, E_L = I_L = E_H = I_H = 0.02$. Such initial conditions match those in the ODE study [9, 10]. The solution curves are shown in Fig. 1. We observe reasonably good agreement with the results obtained by using the ODE model [9, 10].

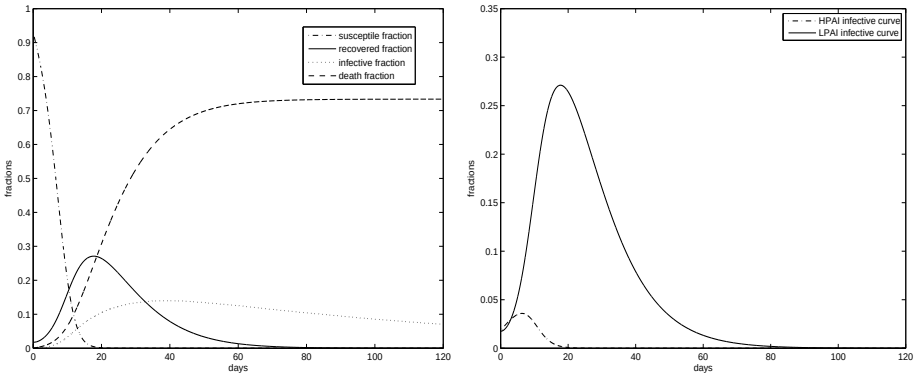

(a) (b)

FIGURE 1. PDE results with very small diffusion coefficient: (a) dynamics of HPAI without mutation, (b) comparison of HPAI and LPAI infection.

4.1.2. Now we set $\varepsilon = 0.1$, representing a moderate diffusive effect, with the same initial conditions as in Sec **4.1.1**. Now, due to the stronger diffusion term, the solution curves are quickly smoothed out and approach to zero values, showing the differences with the ODE results (see Fig. 2).

4.1.3. For yet another validity test, we set $\varepsilon = 0.001$, $I_H = I_L = E_H = E_L = 0.02cos(x - \frac{L}{2})$, $S = 1 - 0.08cos(x - \frac{L}{2})$, and 0 for other variables. Here L is the length of the computational domain. The value of L is not essential and, for simplicity, we set $L = 2$. Although spatial variances are included in the initial profiles, there is almost no change in the results (see Fig. 3) compared with those in Fig. 1, due to the very small value of ε.

4.2. **Bird population dynamics with small initial perturbations.** In avian influenza study, one interesting question is whether a small amount of infected birds will spread the infection to the entire domain (locally or globally) and cause a pandemic. Mathematically, this question is equivalent to what is the consequence of a small initial perturbation to the spatial and temporal dynamics. To explore the answer, we perform the following tests with the initial infection profiles modeled as a Sine wave in the center of the domain. We fix the domain size to $L = 2$, and the diffusion coefficient with a moderate value $\varepsilon = 0.1$. We then study the dynamics of the bird population with such initial conditions. We will add the human population in Section **4.3**.

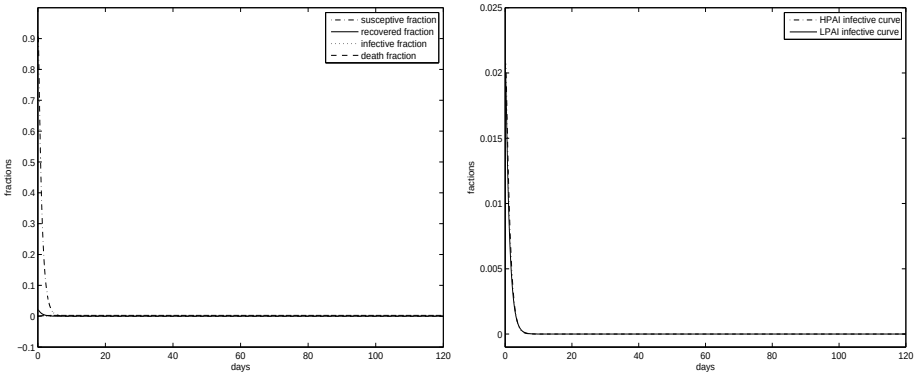

(a) (b)

FIGURE 2. PDE results with bigger diffusion coefficient: (a) dynamics of HPAI without mutation, (b) comparison of HPAI and LPAI infection.

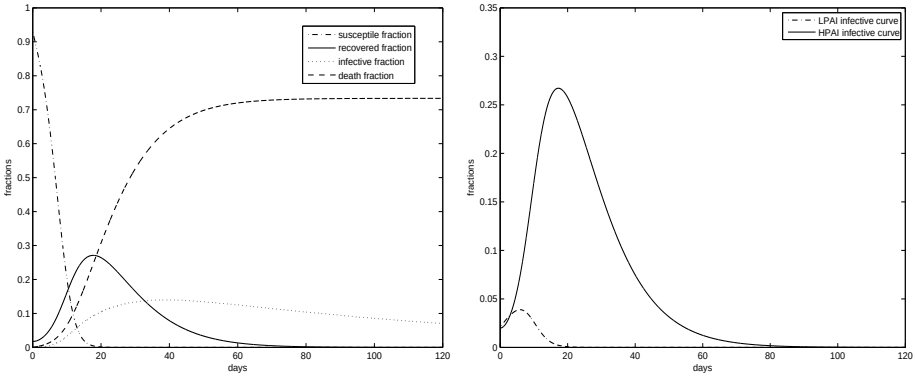

(a) (b)

FIGURE 3. PDE results with very small diffusion coefficient and initial spatial variances: (a) dynamics of HPAI without mutation, (b) comparison of HPAI and LPAI infection.

4.2.1. First, we set, at $t = 0$,

$$I_H = I_L = \begin{cases} 0.04sin(\frac{x-0.8}{0.4}\pi) & : \quad 0.8 < x < 1.2 \\ 0 & : \quad otherwise, \end{cases}$$

$s = 0.92$, and 0 for all other variables.

The solution curves for the recovered and dead birds at $t = 100$ (representing a steady state) are presented in Fig. 4. In particular, we observe that the small initial population of I_H becauses a death rate close to 90% at $t = 100$, indicating a pandemic among birds.

4.2.2. To gain better insight of the effect of the initial value I_H on the death rate, we change the initial wave amplitudes for I_H and I_L as follows. Other initial

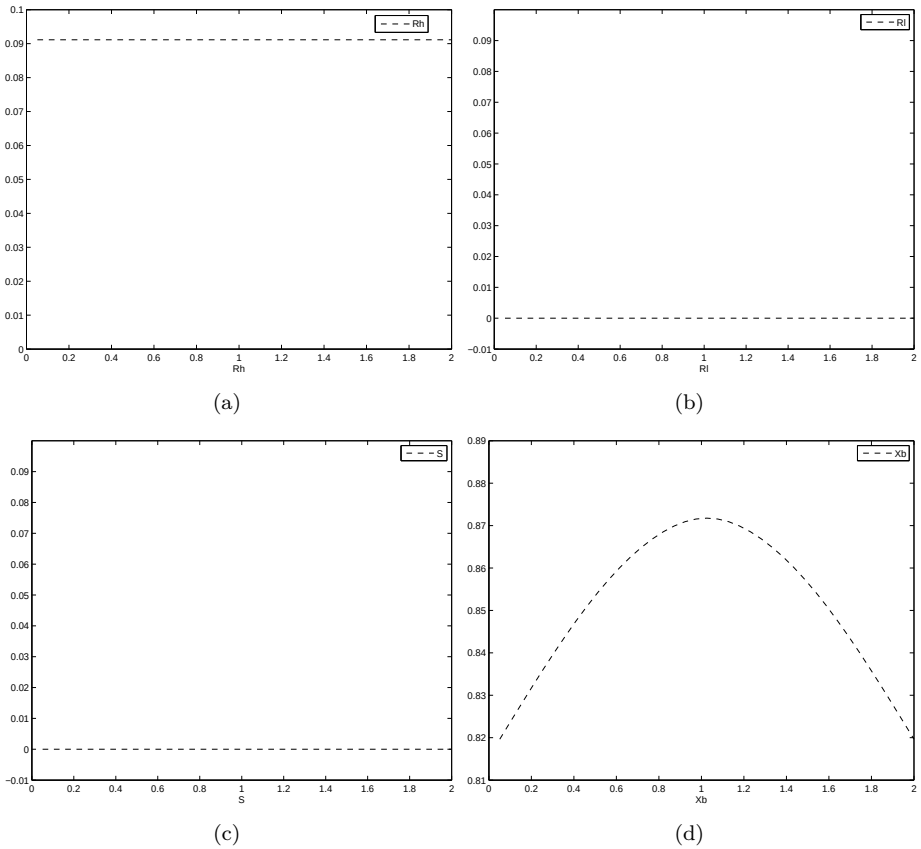

FIGURE 4. The values of the recovered (a and b), susceptible (c) and death (d) rates at t=100.

configurations are the same with those in Sec **4.2.1**.

$$I_H = \begin{cases} 0.01sin(\frac{x-0.8}{0.4}\pi) & : \quad 0.8 < x < 1.2 \\ 0 & : \quad otherwise, \end{cases}$$

$$I_L = \begin{cases} 0.07sin(\frac{x-0.8}{0.4}\pi) & : \quad 0.8 < x < 1.2 \\ 0 & : \quad otherwise, \end{cases}$$

The results are presented in Fig. 5.

The results show that with even smaller initial I_H, the death rate is still about 80% at $t = 100$, and there is no improvement for the recovery rates. This means that HPAI outbreak in birds still occurs. The fundamental reason for such behavior is unclear yet. Within our model, this might be due to the relatively big value of the transmission parameter a_2 which transfers a large portion of the susceptible population (S) into the E_H set. This hypothesis, as well as the reliability of the current value for a_2, can be justified by conducting a sensibility analysis on our model. This would provide an interesting direction for our future research. One evidence to support this hypothesis is presented below with a simple linear test.

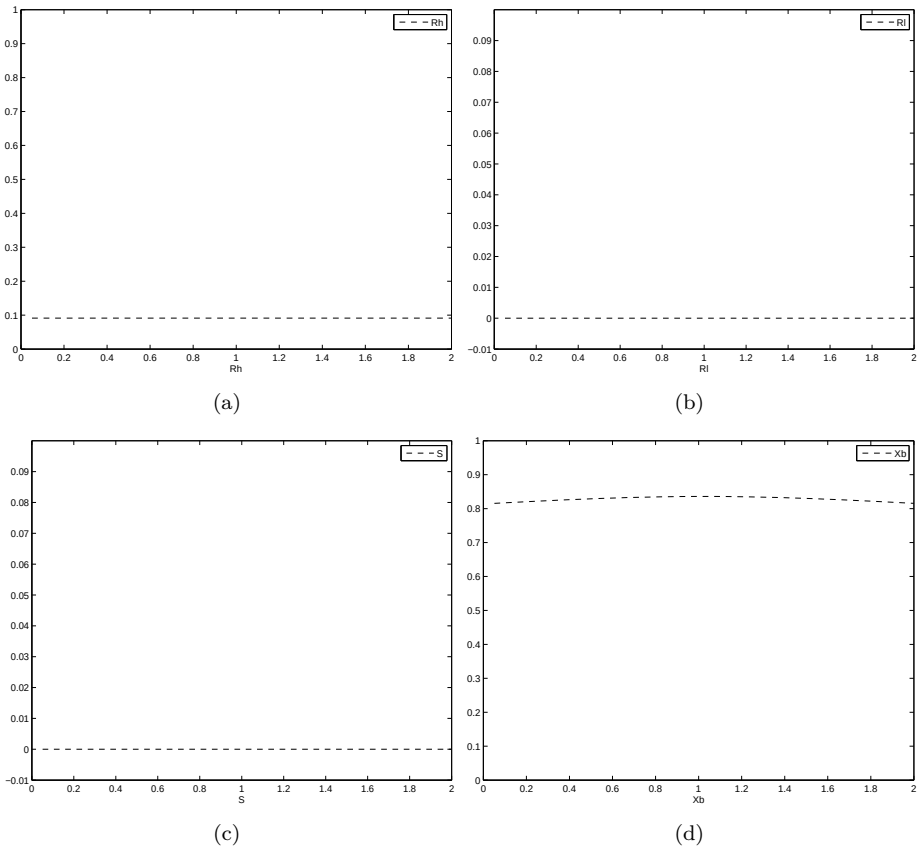

FIGURE 5. The values of recovered (a and b), susceptible (c) and death (d) rates at $t = 100$, with lower value of initial HPAI.

4.2.3. We consider the same initial conditions as in Sec **4.2.1**, and set the parameter values $a_1 = a_2 = a_3 = \tau = \rho = 0$. This would yield the linearized model of our PDE system. Now, due to the absence of nonlinear interaction between different population sets, particularly between S and E_H, both the infection and death rates are extremely low (shown in Fig. 6) and the pandemic does not appear. This pattern exhibits sharp contrast to the nonlinear dynamics.

4.3. **Combined bird and human population dynamics.** Now we add the human part into the model and study the combined dynamics for birds and humans with small amount of initial infections.

4.3.1. For initial profiles of

$$I_H = I_L = \begin{cases} 0.04sin(\frac{x-0.8}{0.4}\pi) & : \quad 0.8 < x < 1.2 \\ 0 & : \quad otherwise, \end{cases}$$

which corresponds to **4.2.1**. We plot the recovered and dead populations again at $t = 100$ (see Fig. 7). The results show that the death rate of the birds is close to 90%, similar to the case without human population. On the other hand, the death

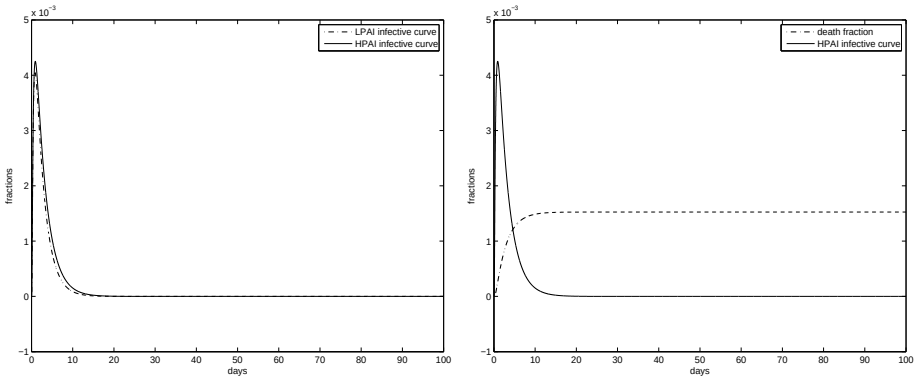

(a) (b)

FIGURE 6. PDE results for the linearized model.

rate of humans is about 9% at $t = 100$. This would certainly be considered as a very serious situation if that happened in the real would.

4.3.2. Finally, we conducted simulation with the initial profiles corresponding to those in **4.2.2**. We observed similar dynamics as those in Sec **4.3.1** and the results are not shown here. This confirms that the infection pattern does not depend on the specific initial configurations, and any small initial infection would lead to a severe disease outbreak.

5. **Conclusion.** In this paper, we have formulated a PDE model and performed computational study on both the temporal and spatial dynamics of Avian Influenza in a combined system of birds and humans. Our results show that even with extremely small amount of initial infection of birds, the HPAI outbreak will occur in birds, killing as high as 90% of the total bird population. Meanwhile, this will cause very serious infection which leads to a considerable death rate among human beings. Based on our model, such epidemic behaviors cannot be eliminated or even controlled by the system itself.

Given these findings, external control strategies (such as vaccination and culling infected birds) have to be enforced to save human and bird lives, and to limit the scope of the infection as much as possible. Our model does not consider the effects of such external controls, but this would be an interesting topic for our future study. In addition, the extension of our model to two-dimensional and three-dimensional cases is expected to produce more realistic results.

Acknowledgments. The authors would like to thank the two anonymous referees for their helpful suggestions to improve this paper.

REFERENCES

[1] D. A. Anderson, J. C. Tannehill and R. H. Pletcher, "Computational Fluid Mechanics and Heat Transfer," Hemisphere Publishing Corporation, 1984.

[2] S. Deckelman and J. P. Tian, *A case study of disease ecology: Modeling of avian flu*, preprint, (2010).

[3] V. D. Goot et al., *Comparison of the transmission characteristics of low and high pathogenicity avian influenza A virus (H5N2)*, Epidemiological Infections, **131** (2003), 1003–1013.

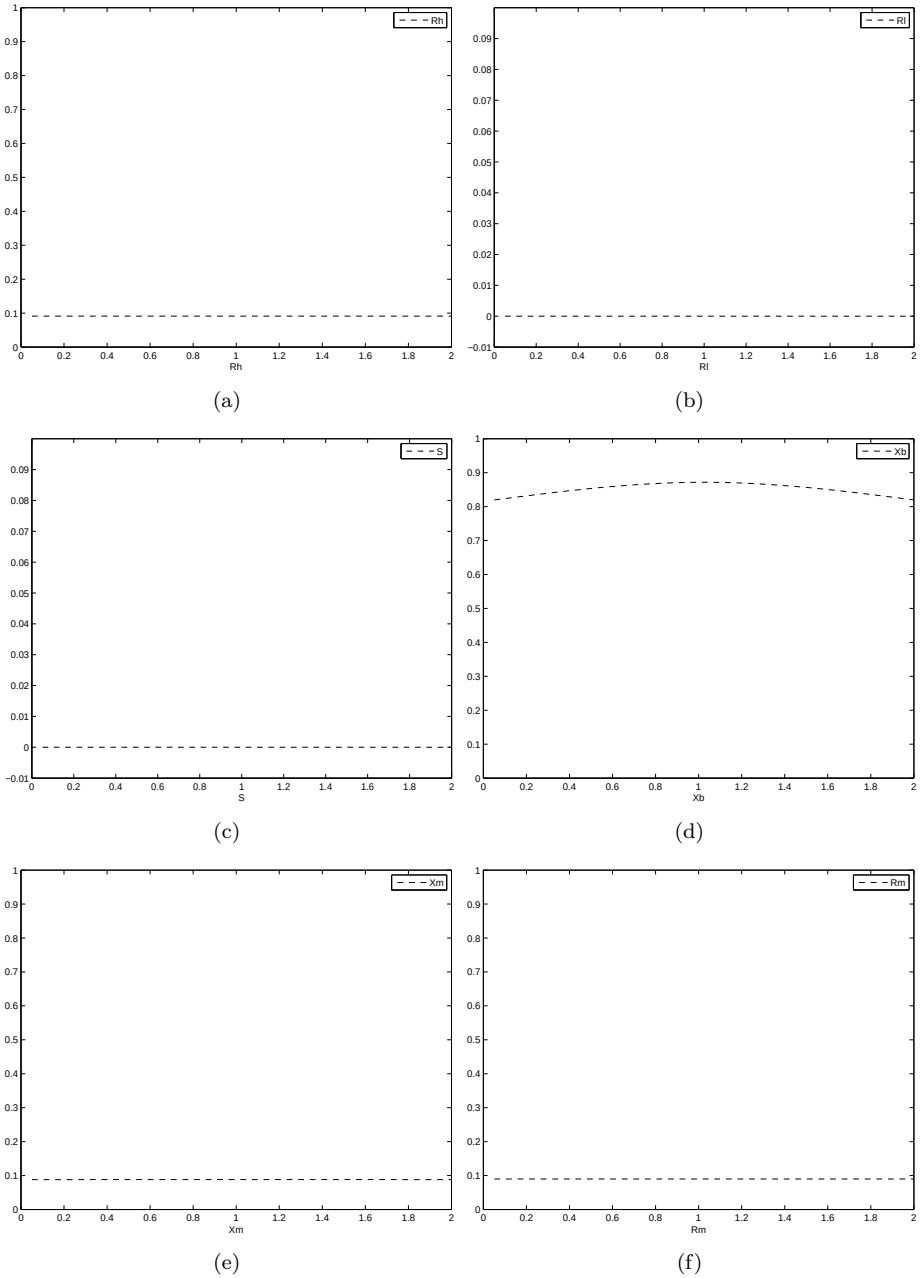

FIGURE 7. The recovered and death rates in the combined bird and human system.

[4] T. Horimoto and Y. Kawaoka, *Pandemic threat posed by avian influenza A viruses*, Clinical Microbiology Reviews, Jan., (2001), 129–149.
[5] T. Ito, et al, *Generation of a highly pathogenic avian influenza A virus from an avirulent field isolated by passaging in chickens*, The Journal of Virology, (2001), 4439–4443.

[6] M. Lewis, J.Renclawowicz and P. v. d. Driessche, *Traveling waves and spread rates for a West Nile virus model*, Bulletin of Mathematical Biology, **68** (2006), 3–23.
[7] B. Olsen et al., *Global patterns of influenza A virus in wild birds*, Science, **312** (2006), 384–388.
[8] R. R. Rogoes and S. Bonhoeffer, *Emergence of drug-resistant influenza virus: Population dynamics considerations*, Science, **312** (2006), 389–391.
[9] J. Shi, J. P. Tian and X. Hou, *A model for emergence of high pathogenicity avian influenza virus from outbreaks with low pathogenicity avian influenza virus*, preprint, (2010).
[10] J. P. Tian, *Case study of disease ecology: Avian influenza a virus, international symposium on ecology*, Evolution and Modeling of Disease Dynamics, Beijing, China, (2007).
[11] *World health organization web page: www.who.org.*
[12] *Center for disease control and prevention web page: www.cdc.gov.*

Received April 2009; revised October 2009.

E-mail address: ywm2006@yahoo.com
E-mail address: j3wang@odu.edu
E-mail address: jptian@math.wm.edu